ACADEMIC PRESS

Available online at www.sciencedirect.com
SCIENCE DIRECT®

Journal of Catalysis 215 (2003) 66–77

JOURNAL OF CATALYSIS

www.elsevier.com/locate/jcat

Effect of zirconia-modified alumina on the properties of $Co/\gamma\text{-}Al_2O_3$ catalysts

Bunjerd Jongsomjit,[1] Joongjai Panpranot,[1] and James G. Goodwin Jr. *

Department of Chemical Engineering, Clemson University, Clemson, SC 29634, USA

Received 15 April 2002; revised 4 November 2002; accepted 7 November 2002

Abstract

Zr promotion has been shown to improve the activity of Co/SiO_2 and Co/Al_2O_3 Fischer–Tropsch synthesis (FTS) catalysts. However, little is known about how it works. The focus of this study was to investigate the impact of Zr modification of alumina used to support Co catalysts. Zr was first impregnated into alumina to produce Zr-modified alumina supports containing 2–11 wt% of ZrO_2 in the final catalyst. Co catalysts having 20 wt% Co were then prepared from these supports by incipient wetness. It was found that Zr modification had a significant impact on the catalyst properties: FTS rate per gram of catalyst increased significantly (> 65% at steady state) with Zr modification and Co reducibility, especially during standard reduction, also increased. H_2 chemisorption, however, was found to be essentially constant with Zr modification. The impact of Zr modification is likely due to stabilization of the alumina support, prevention or blockage of Co surface "aluminate" formation, and an increase in Co reducibility to the active catalytic metallic phase. SSITKA results for CO hydrogenation showed an increase in the number of active surface intermediates (N_M) with Zr modification while the intrinsic activity ($1/\tau_M$) remained constant, confirming that the major impact of Zr was in increasing the concentration of active Co surface sites. Because of the inconsistency of the turnover frequency calculated based on H_2 chemisorption with the $1/\tau_M$ results, it is suggested that the standard adsorption conditions usually used for Co may not be adequate for modified Co catalysts such as the ones studied here.

Keywords: Zr modification; Co FTS catalysts; CO hydrogenation; Co-support compound formation

1. Introduction

To increase catalyst activity, many promoters such as Ru [1–3], Zr [4,5], La [6], Rh [7–9], B [10], and Pt [11] have been investigated for Co catalysts. It has been proposed that a variety of these promoters can increase the reducibility of Co, preserve the activity by preventing the formation of coke, exhibit cluster and ligand effects, act as a source of hydrogen spillover, and enhance the dispersion. The use of additives to specifically modify the metal–support interaction has also been investigated. It has been found that metal dispersion, chemical state, as well as catalyst activity are affected by changing the interaction between the metal catalytic phase and the support as a result of modification using B, Ge, Ga, and Zn [10,12–20].

It has been shown that cobalt-support compound formation (Co-SCF) in cobalt-based catalysts, especially those used in Fischer–Tropsch synthesis (FTS), can occur during pretreatment and/or under reaction conditions [21–34]. This irreversible Co-SCF causes a decrease in the overall catalyst activity due to the loss of active Co metal available for catalyzing the reaction.

A number of FTS patents by Shell [35,36] have involved Zr promotion of Co/SiO_2. Ali et al. [4] investigated Zr promotion of Co/SiO_2 catalysts for FTS and found that Zr is basically a rate promoter. Rohr et al. [5] investigated the effect of adding Zr to an alumina support for Co FTS catalysts. They found that, at 5 bar and a $H_2:CO$ ratio of 9 : 1, Zr-modified alumina-supported Co exhibited an increase in the activity and selectivity to C_{5+} hydrocarbons. Steady-state isotopic transient kinetic analysis (SSITKA) showed that the intrinsic activity of Co/Al_2O_3 was not greatly affected by Zr modification [5]. Although Zr modification appears to increase the rate of FTS on Co catalysts [4,5], no studies have specifically addressed how Zr promotes the reaction. Under-

* Corresponding author.
E-mail address: james.goodwin@ces.clemson.edu (J.G. Goodwin Jr.).
[1] Department of Chemical Engineering, Chulalongkorn University, Phyathai Road, Bangkok 10330, Thailand.

0021-9517/03/$ – see front matter
doi:10.1016/S0021-9517(02)00102-1

standing how Zr modifies catalyst properties could lead to the design of more robust and active Co catalysts.

This investigation focused on studying the impact of Zr modification of Co/γ-Al_2O_3 catalysts. A series of Co/γ-Al_2O_3–Zr catalysts were prepared with a range of Zr concentrations. Since the presence of water vapor during reduction is known to increase Co–aluminate formation, the impact of Zr loading on the reducibility of Co in the absence and presence of water vapor was investigated. The effect on the reaction rate and product distribution during FTS was also measured. SSITKA of CO hydrogenation was performed to obtain a better understanding of the effect of Zr modification on the intrinsic activity and surface coverage of reaction intermediates.

2. Experimental

2.1. Materials

2.1.1. Co/γ-Al_2O_3

The Co/γ-Al_2O_3 catalyst was prepared by the incipient wetness impregnation of γ-Al_2O_3. The support precursor (Al_2O_3, Vista B) was first calcined at 500 °C for 10 h before impregnation to put it in the form of γ-Al_2O_3 having a specific surface area of 209 m^2/g and average particle size of ca. 60 μm. Cobalt nitrate [$Co(NO_3)_2 \cdot 6H_2O$] was dissolved in deionized water and impregnated into the support using incipient wetness to give a final catalyst with 20 wt% cobalt. The catalyst was dried at 110 °C for 12 h and calcined in air at 300 °C for 2 h following a ramp to temperature at 1 °C/min.

2.1.2. Co/γ-Al_2O_3–Zr

The Zr-modified alumina-supported Co catalysts (Co/γ-Al_2O_3–Zr) were prepared by the sequential impregnation method. The same support (γ-Al_2O_3) as mentioned above was used. First, Zr was impregnated into the support using a solution of zirconium(IV) *n*-propoxide (70 wt% in *n*-propanol, Alfa Aesar) to produce Zr-modified alumina supports having 2, 5, and 11 wt% of ZrO_2. Second, the Zr-modified supports were calcined at 350 °C for 2 h (ramp rate 1 °C/min) prior to impregnation of cobalt.

Cobalt nitrate was used to impregnate the Zr-modified supports to produce calcined catalysts with 20 wt% cobalt using the same procedure as given in the previous section.

2.2. Catalyst pretreatment and nomenclature

Standard reduction was carried out at 350 °C for 10 h in flowing hydrogen after ramping to temperature at 1 °C/min to reduce the Co to its active state for reaction. The catalysts were characterized following these three pretreatments:

(i) The original calcination step;

Table 1
Catalyst compositions

Catalyst samples	Compositions (wt%)		
	Co	ZrO_2	γ-Al_2O_3
Co/Al	20	0	80
Co/Al–Zr-02	20	2.2	77.8
Co/Al–Zr-05	20	5.4	74.6
Co/Al–Zr-11	20	10.8	69.2

(ii) Standard reduction of the calcined catalysts at 350 °C using a high space velocity (16,000 h^{-1}) of H_2 followed by passivation with an O_2/He (5.20% of O_2) mixture at room temperature for 2 h;

(iii) Standard reduction of the calcined catalysts at 350 °C using a high space velocity (16,000 h^{-1}) of a mixture of H_2 and 3 vol% water vapor followed by passivation with an O_2/He (5.20% of O_2) mixture at room temperature for 2 h.

The nomenclature used for samples in this study is the following:

$$\boldsymbol{Co/Al–Zr\text{-}n\text{-}i},$$

where $\boldsymbol{n}$ refers to wt% ZrO_2 in the support; $\boldsymbol{i = C}$ refers to the calcined catalyst samples; $\boldsymbol{i = RP}$ refers to the reduced and passivated catalyst samples; $\boldsymbol{i = R_WP}$ refers to the samples reduced in the presence of 3 vol% water vapor and then passivated.

The catalyst compositions are shown in Table 1.

2.3. Catalyst characterization

2.3.1. X-ray powder diffraction (XRD)

XRD was performed to determine the bulk crystalline phases of the catalysts following different pretreatment conditions. X-ray powder diffraction patterns of samples were collected using a Scintag XDS-2000 X-ray diffractometer with monochromatized Cu-K_α radiation ($\lambda = 1.54439$ Å). The spectra were scanned at a rate of 2.4°/min from $2\theta = 20$ to 80°.

2.3.2. Raman spectroscopy

The Raman spectra of the samples were collected by projecting a continuous wave laser of helium–neon (He–Ne) red (632.816 nm) through the samples exposed to air at room temperature. A scanning range between 100 and 1000 cm^{-1} with a resolution of 2 cm^{-1} was applied. The data were analyzed using Renishaw WiRE (Windows-based Raman Environment) software, which allowed Raman spectra to be captured, calibrated, and analyzed using system 2000 functionality via the Galactic GRAMS interface with global imaging capacity.

2.3.3. SEM and EDX

SEM and EDX were performed to study the morphologies of the catalyst samples and their elemental distributions,

respectively. A Hitachi S3500N SEM was used in the backscattering electron (BSE) mode at 15 kV with a working distance (the distance between a sample and the electron beam) of 15 mm. After the SEM micrographs were taken, EDX was performed to determine the elemental concentration on the catalyst surface (using INCA software).

2.3.4. Hydrogen chemisorption

Static H_2 chemisorption on the re-reduced cobalt catalyst samples at 100 °C was performed using the method described by Reuel and Bartholomew [37] and was used to determine the number of reduced cobalt metal surface atoms. This is usually related to the overall activity of the catalyst during FTS. Chemisorption was conducted in a Micromeritics ASAP 2010 and analyzed using ASAP 2010C V3.00 software. Prior to H_2 chemisorption, the reduced and passivated catalyst samples were evacuated to 10^{-6} mm Hg at 100 °C for 15 min, reduced in flowing H_2 (50 cc/min) at 100 °C for 15 min, reduced at 350 °C in flowing H_2 for 10 h, and then evacuated at 350 °C for 90 min to desorb any hydrogen.

2.3.5. Temperature-programmed reduction (TPR)

TPR was performed to determine the reducibility and reduction behavior of the catalyst samples. TPR was carried out in an Altamira AMI-1 system using 50 mg of catalyst and a temperature ramp from 30 to 800 °C at 5 °C/min. The reduction gas was 5% H_2 in Ar. A cold trap (−70 °C) was placed before the detector to remove water produced during the reaction. A thermal conductivity detector (TCD) was used to determine the amount of hydrogen consumed. The hydrogen consumption was calibrated using TPR of silver oxide (Ag_2O) at the same conditions. The reduced and passivated catalyst samples were re-calcined in situ at 300 °C for 2 h before TPR was performed.

2.4. Reaction

FTS was carried out under differential reaction conditions (< 5% conversion) at 220 °C and 1 atm total pressure. A flow rate of $H_2/CO/Ar = 60/30/10$ cc/min in a fixed-bed reactor under differential reaction conditions was used. Thermocouples at the top and the bottom of the catalyst bed ensured precise temperature control during pretreatment and reaction. Typically, 0.2 g of the pretreated catalyst sample was re-reduced in situ in flowing H_2 (50 cc/min) at 350 °C for 10 h prior to FTS. To avoid exotherms and hot spots that lead to rapid catalyst deactivation, the reaction was initiated in a controlled manner by gradually increasing the reactant concentrations over a period of 2 h. After the start-up, samples were taken in 3-h intervals and analyzed by on-line gas chromatography. Steady state was reached after 24 h in all cases.

2.5. Steady-state isotopic transient kinetic analysis (SSITKA)

SSITKA was performed using a differential fixed-bed glass microreactor. Hydrogenation of CO was carried out at 220 °C and 1.8 atm. A flow rate of $H_2/CO/He = 20/2/8$ cc/min was used. A relatively high H_2/CO ratio of 10 was used to minimize deactivation due to carbon deposition during reaction. Thermocouples at the top and at the bottom of the catalyst bed assured precise temperature control during pretreatment and reaction. Typically, 15 mg of a calcined catalyst sample was re-reduced in situ in flowing H_2 (30 cc/min) at 350 °C for 10 h prior to the reaction. As the reaction began, reactor effluent samples were taken at 1-h intervals and analyzed by on-line GC. Generally, steady state was reached after 5 h in all cases. During steady state, transients of methane and CO were obtained by switching the inlet flow of $^{12}CO/Ar$ to ^{13}CO without disturbing the stability of the reaction. A trace (5%) of Ar in the ^{12}CO was used to account for the gas-phase holdup of the system. The decay or increase of isotopically marked species was monitored by an on-line Leybold-Inficon Auditor-2 quadruple mass spectrometer. Average surface residence times for the carbon in CH_4 and CO were calculated from these transient studies. The number of surface intermediates which gave rise to CH_4 and the amount of reversibly chemisorbed CO were also calculated.

3. Results

3.1. X-ray diffraction

XRD patterns for the calcined Co catalysts (with and without Zr modification) and Co_3O_4 (spinel) are shown in Fig. 1. They had identical XRD patterns. The diffraction peaks at 31.3°, 36.8°, 45°, 55°, 59.4°, and 65.4° are those of Co_3O_4. Peaks for γ-Al_2O_3 were also evident. No peaks of ZrO_2 or any other Zr compound, however, were detected. This indicates that Zr was present in a highly dispersed form [4]. It will be assumed from this point on in the paper that Zr was in the form of ZrO_2. After reduction and passivation, only XRD peaks of CoO (at 37°, 42.6°, and 61.8°) and γ-Al_2O_3 were evident. No Co metal peaks were seen due to its high dispersion and their overlap with those for γ-Al_2O_3. No XRD peaks of $CoAl_2O_4$ (spinel) [38] could be detected either for any of the catalyst samples. Recalcination of the reduced catalysts caused the cobalt to revert back to Co_3O_4.

3.2. Raman spectroscopy

Raman spectra for the calcined catalyst samples and Co_3O_4 are shown in Fig. 2. After calcination, Raman bands at 198, 480, 519, 619, and 690 cm^{-1} were observed for all calcined catalyst samples. These can be best assigned to

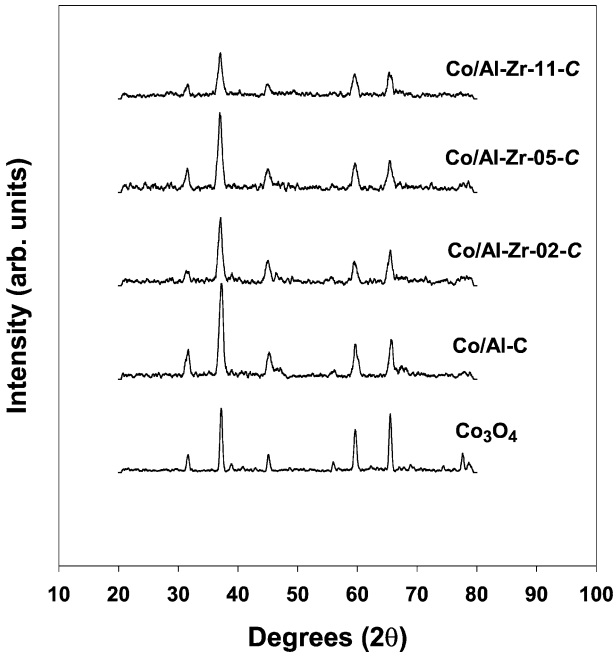

Fig. 1. XRD patterns of Co_3O_4 and the calcined Co catalysts.

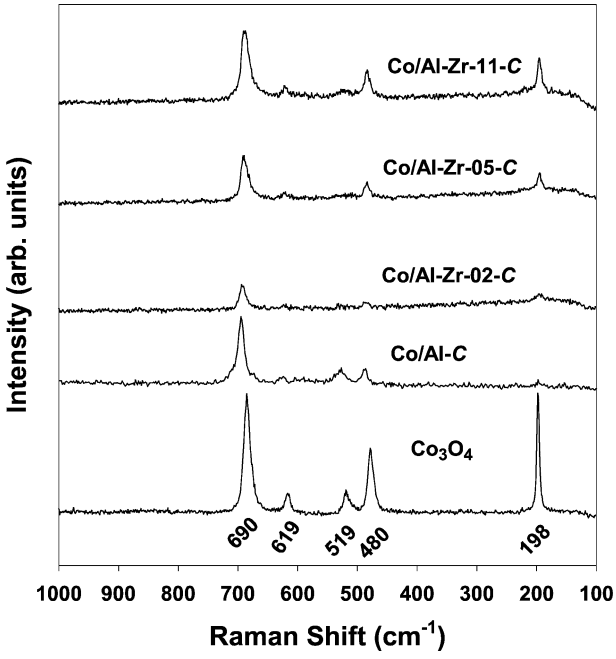

Fig. 2. Raman spectra of Co_3O_4 and the calcined catalysts.

Co_3O_4. The Raman spectrum for γ-Al_2O_3 was essentially flat. The Raman band (at 642 cm^{-1}) for ZrO_2 [39] was not seen for any of the catalyst samples. Raman spectra of the reduced and passivated catalyst samples are shown in Fig. 3. Raman bands for all reduced and passivated catalyst samples with Zr modification were identical, but different from those for the reduced and passivated Co catalyst without Zr modification (Co/Al-***RP***). Only two very broad Raman bands at ca. 690 and, especially, 560 cm^{-1} were detected for Co/Al-***RP*** and this has been correlated to the formation of a

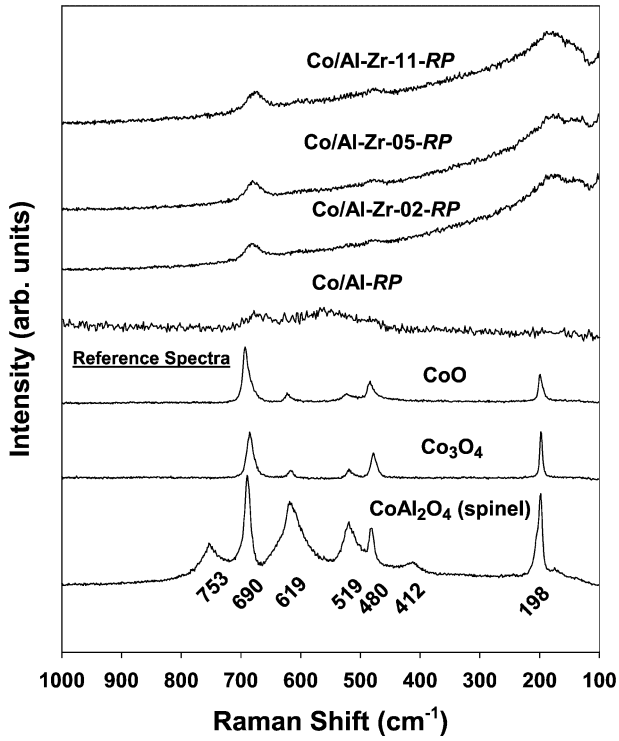

Fig. 3. Raman spectra of CoO, Co_3O_4, $CoAl_2O_4$ (spinel), and the reduced and passivated catalysts.

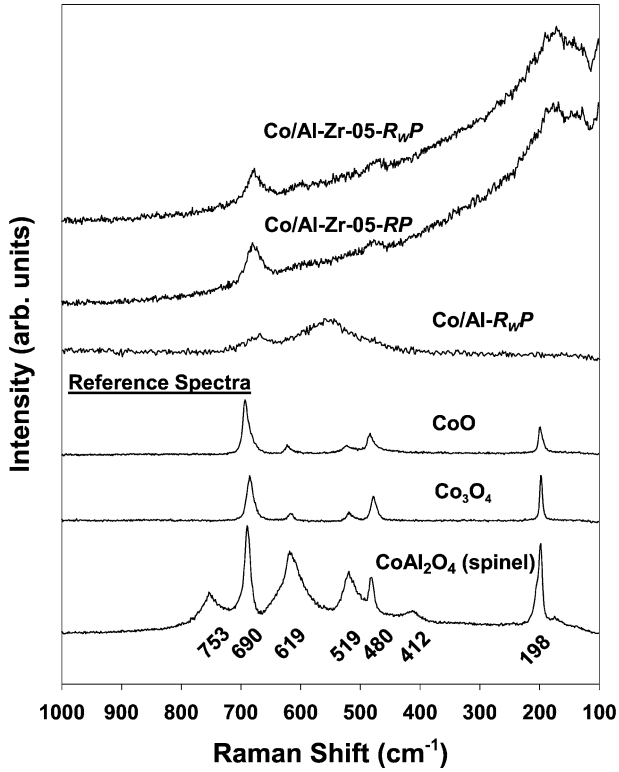

Fig. 4. Raman spectra of CoO, Co_3O_4, $CoAl_2O_4$ (spinel), and the reduced (with 3% H_2O vapor added) and passivated catalysts. The spectrum for Co/Al–Zr-05-***RP*** is included for reference.

highly dispersed Co "aluminate" phase [38]. Similar results, except stronger bands, can be observed for the Co/Al sample reduced with 3 vol% added water vapor (***$R_W P$*** samples) as shown in Fig. 4. Strong Raman bands at 690, 480, and 198 cm^{-1} were observed for the reduced and passivated catalyst samples with Zr modification (***RP*** and ***$R_W P$***, Figs. 3 and 4). These bands can best be assigned to Co_3O_4, present on the Co surface after the samples were passivated and exposed to air, rather than CoO (detected in the bulk by XRD) since Raman is more of a surface technique. There was also little evidence of much formation of the highly dispersed Co "aluminate" phase [38] for the Zr-modified catalysts. No peaks for $CoAl_2O_4$ (spinel) were detected in any of the samples.

3.3. SEM and EDX

The typical external particle/granule morphologies of the calcined catalyst samples are shown in Fig. 5. In all the Co catalyst micrographs, the white or light spots on the external surfaces represent high concentrations of Co and its compounds and the gray areas represent the alumina or Zr-modified alumina support with no/minimal Co present. There was no significant change in morphology between the alumina and Zr-modified alumina supports. However, it can be seen in Fig. 5 that Co on the Zr-modified alumina supports was better distributed (i.e., had smaller SEM–visible Co patches/particles that were more scattered) than on the unmodified alumina support.

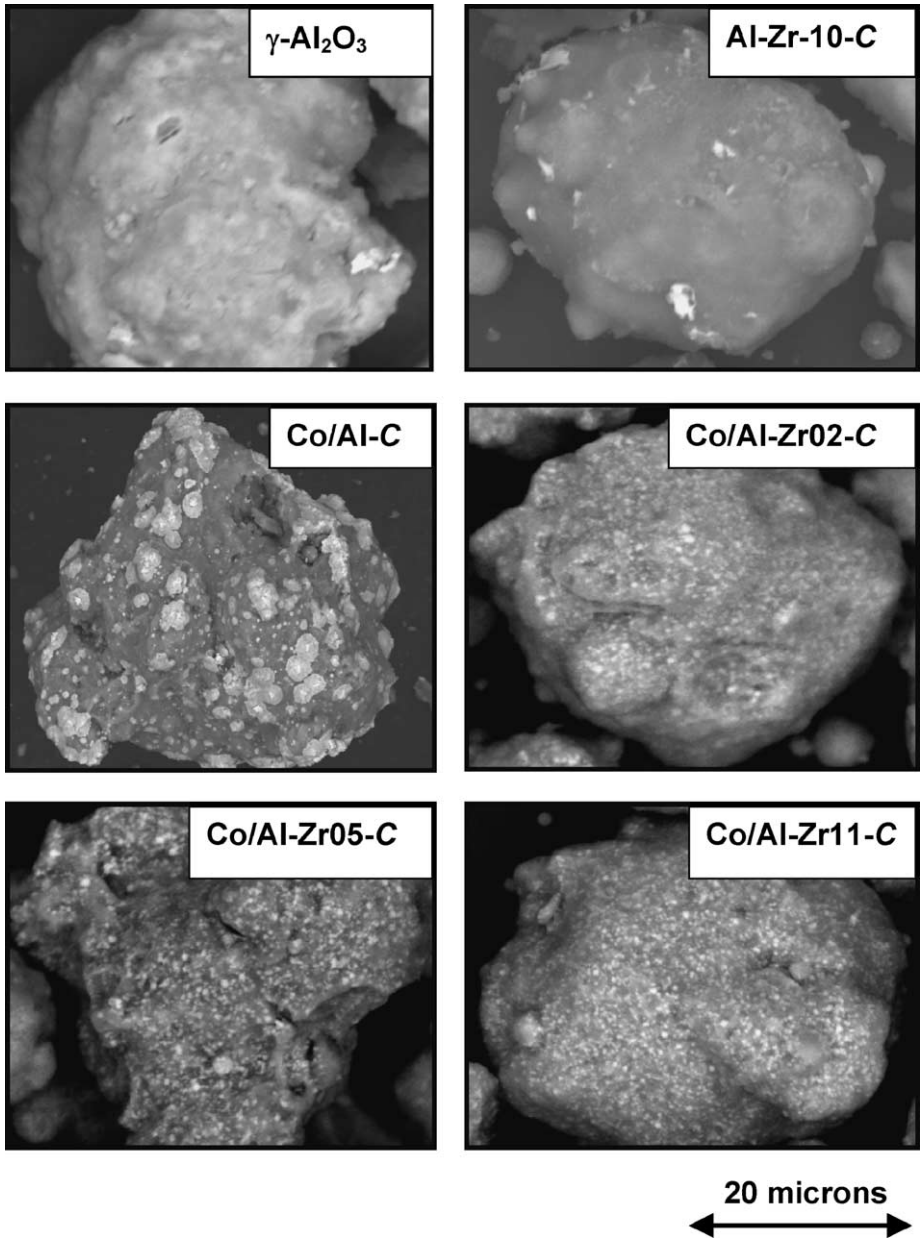

Fig. 5. SEM micrographs of catalyst granules.

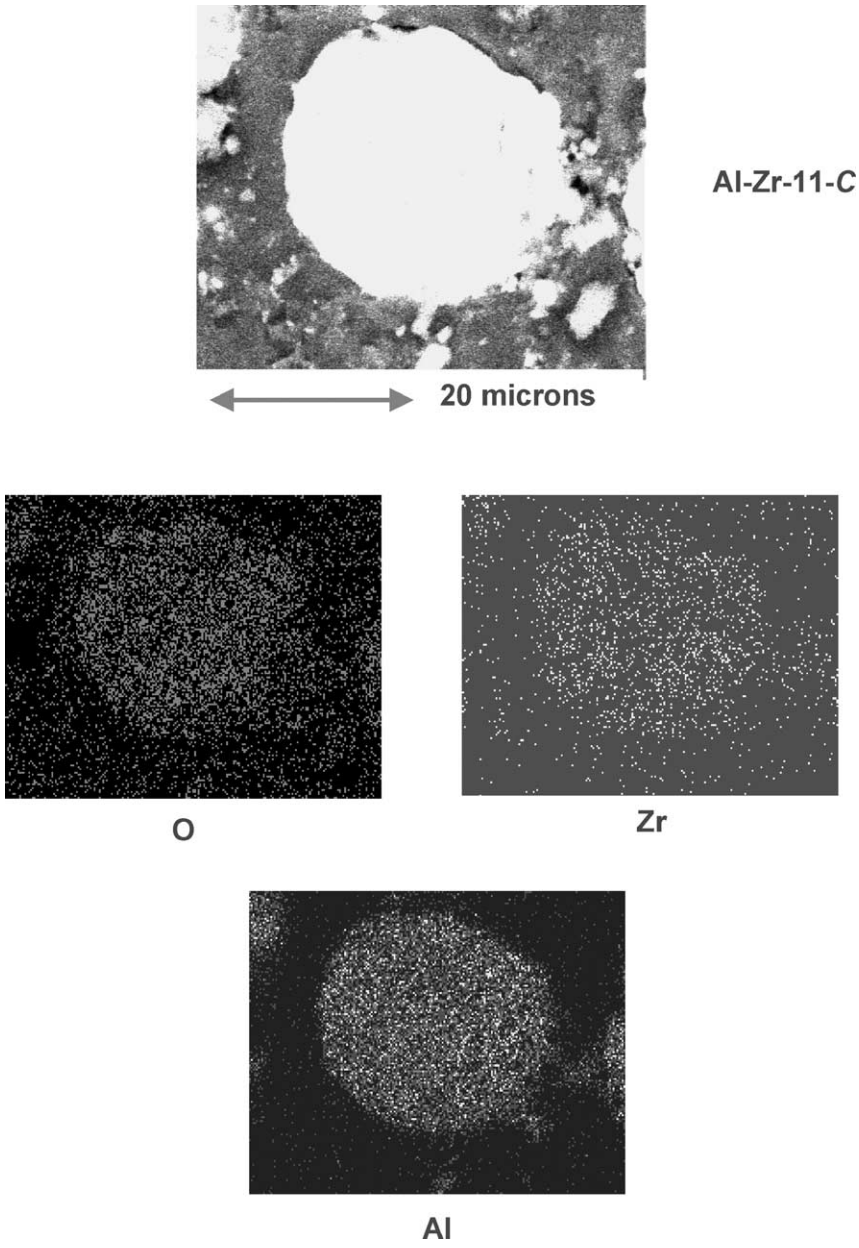

Fig. 6. SEM micrograph and EDX mapping of a calcined Al–Zr-11-***C*** support granule (cross section).

EDX gave useful information about the elemental distribution on the cross-sectioned calcined catalyst granules, i.e., in the catalyst granule interiors. Figure 6 shows the typical elemental distribution for a cross section of a granule of Zr-modified alumina support. EDX mapping indicated that all elements in the modified support were well distributed throughout the catalyst granules. This was also true for the catalyst after Co loading, as shown in Fig. 7.

3.4. Temperature-programmed reduction (TPR)

To eliminate residual $Co(NO_3)_2$ and its impact on the TPR spectra and the calculation of reducibility [38], all TPR results are reported after initial reduction and re-calcination at 300 °C (Fig. 8). There were two major peaks for Co/Al-***C*** located at ca. 350 °C and between 400 and 700 °C (maximum at 600 °C). These peaks have been related to the following reduction steps: $Co_3O_4 \rightarrow CoO$ and $CoO \rightarrow$ Co metal (ca. 350 °C), and Co_XO_Y–$Al_2O_3 \rightarrow$ Co metal (between 400 and 700 °C), respectively [3,11,38,40,41].

There were also three major peaks for the Co catalysts with Zr modification located at 320–350 °C and between 500 and 800 °C (maximum at ca. 700 °C). It would appear that the broad peak with its maximum ca. 600 °C was shifted about 100 °C higher with Zr modification. This indicates that Zr modification caused changes in reduction behavior of the Co catalysts. There was an apparent decrease in both peak locations for the Zr-modified catalysts with Zr loading.

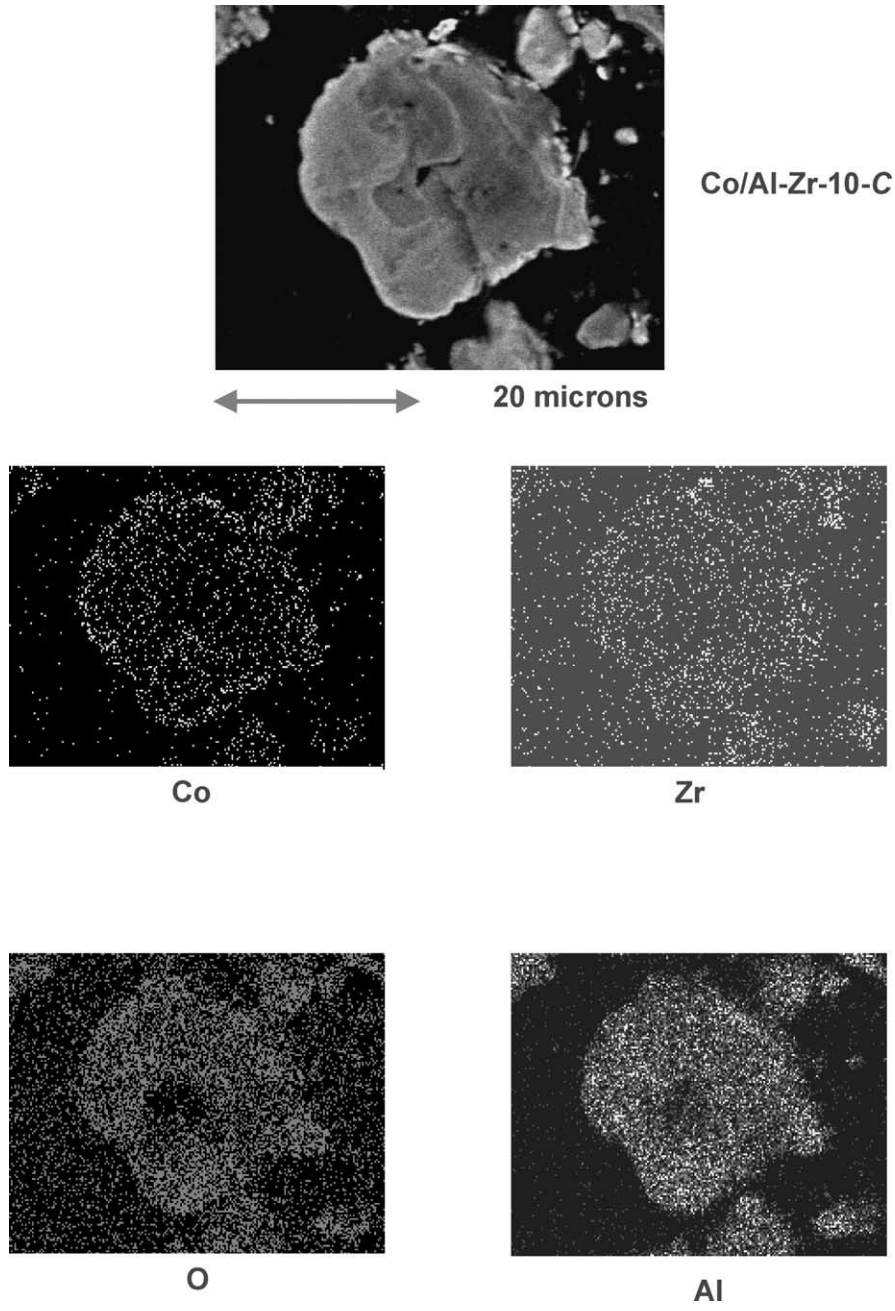

Fig. 7. SEM micrograph and EDX mapping of a Co/Al–Zr-11-***C*** catalyst granule (cross section).

The TPR profile for the Zr-modified support [11 wt% ZrO_2–Al_2O_3 (without Co)] showed no reduction peak. Thus, the support would appear not to have been reducible during TPR. However, one might ask what is the possibility that Co impregnated into the Zr-modified supports can activate hydrogen to partially reduce ZrO_2 as a result of spillover. If that happened, any additional H_2 consumed by ZrO_2 would lead to an overestimation of Co reducibility. To answer this question, TPR of alumina and modified supports containing 5 wt% Pt were studied. All the PtO_2 on alumina was reducible at temperatures 30–400 °C (maximum at 200 °C). While the addition of Zr resulted in a shift of the second reduction peak to higher temperature, there was no evidence for any additional consumption of H_2. Thus, it is concluded that, during TPR, activation of H_2 by reduced Pt or Co was not sufficient to cause any significant reduction of ZrO_2.

Figure 9 shows TPR profiles of the Co/Al and Co/Al–Zr-05 catalysts after reduction with and without added water vapor. These catalysts had been re-calcined prior to TPR. The two-peak reduction TPR profiles were observed for the ***R_WPC*** samples. However, water vapor present during standard reduction resulted in a shift of the second TPR reduction peak to even higher temperature for both the unmodified and Zr-modified catalysts.

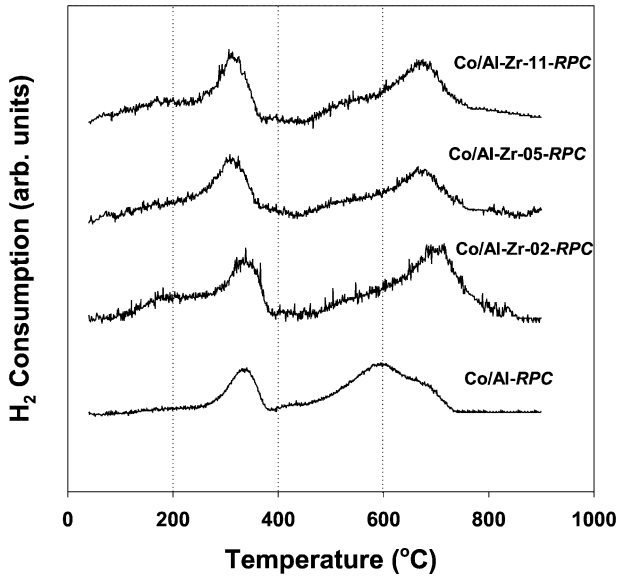

Fig. 8. TPR profiles of the reduced and recalcined catalysts.

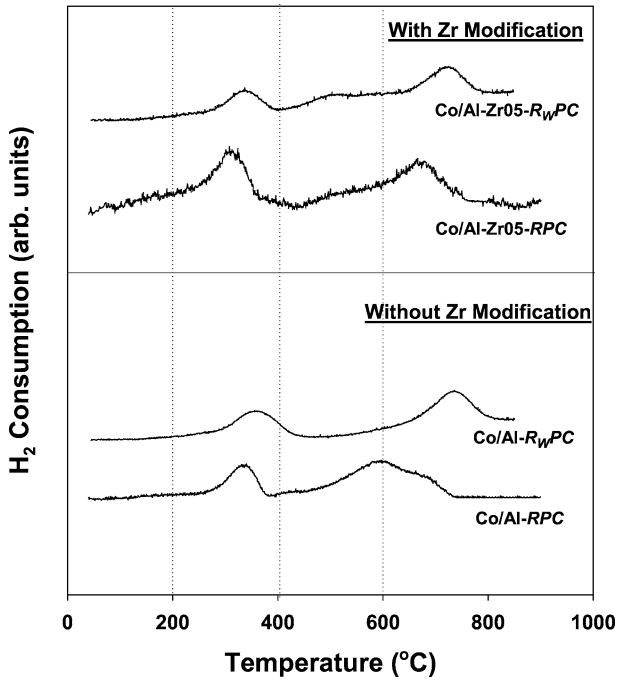

Fig. 9. TPR profiles of recalcined Co/Al and Co/Al–Zr-05 catalysts after reduction with and without added water vapor.

The reducibilities of $Co/\gamma\text{-}Al_2O_3$ and Co on Zr-modified $\gamma\text{-}Al_2O_3$ after various pretreatments are shown in Table 2. While the reducibilities during TPR to 800 °C are interesting, the amount of reduction during TPR from 30 to 400 °C is more important since it is related to the reducibilities of these Co catalysts during standard reduction at 350 °C [23]. It can be seen that the reducibility of alumina-supported Co increased significantly with Zr modification.

3.5. H_2 chemisorption

H_2 chemisorption results are shown in Table 2. The overall dispersion of reduced Co in the catalyst samples based on the H_2 chemisorption results is also given. The Co metal dispersions of the catalysts ranged between 3.5 and 3.8%. The results indicate that the amount of adsorbed H_2 was not dramatically changed with Zr modification, although there was perhaps a slight increase. The Zr-modified support [11 wt% $ZrO_2/\gamma\text{-}Al_2O_3$ (without Co)] was inactive for H_2 chemisorption.

3.6. Reaction rate

FTS was performed to determine the overall activity and product distribution of the Co catalysts with and without Zr modification. The results are shown in Table 3 and Fig. 10. It can be seen that the presence of ZrO_2 (2–11 wt%) as a support modifier increased significantly both the initial and the steady-state FTS rates, $> 115\%$ and $> 65\%$, respectively. TOF based on H_2 chemisorption also increased by approximately 50–100% with Zr modification due to the increase in rate, since the amount of H_2 adsorbed was essentially constant. Considering the product distribution, it can be observed that the addition of the Zr modifier resulted in a slight increase in the Anderson–Schulz–Flory (ASF) chain-growth probability (α). The hydrocarbons formed were primarily straight chain alkanes, typical for Co FTS catalysts at these conditions. As also seen in Table 3, it appears that the amount of carbon deposited on the catalysts during FTS for 24 h (a primary cause of Co deactivation during FTS) decreased with Zr modification. The reaction rates on the unmodified and Zr-modified catalysts after various pretreatments are shown in Table 4. It is obvious that the rate on the initially reduced samples ($-\boldsymbol{R}$) was higher that than on the reduced and passivated samples ($-\boldsymbol{RPR}$ and $-\boldsymbol{R_WPR}$, re-reduced prior to FTS). Moreover, the rate on the reduced and passivated samples decreased with the addition of water vapor during standard reduction (again re-reduced prior to FTS), although less so on the Zr-modified catalyst.

3.7. SSITKA

Steady-state isotopic transient kinetic analysis was used to determine in situ surface reaction parameters. SSITKA enables one to calculate the surface concentration of reaction intermediates and pseudo-first-order rate constant (k_p) [2,6,42]. During steady-state reaction, the surface residence times (τ) for CO and CH_4 were determined by integrating the areas between the transient curves for Ar and labeled CO or CH_4, respectively. The pseudo-first-order rate constant (k_p), a measure of intrinsic site activity for methanation, was calculated by taking the inverse of the residence time of CH_4. The method used to calculate these parameters is described extensively by Shannon and Goodwin [42].

Table 2
Reducibility and H_2 chemisorption results

Catalyst samples	Zr/Co atom ratio	Reducibility[a,b,c]						Chemisorption	
		(30–800 °C)			(30–400 °C)[d]			Total H_2 chemisorption[e] (μmol of H_2/g cat)	% Co dispersion[f]
		C	***RPC***	***R_WPC***	***C***	***RPC***	***R_WPC***		
Co/Al	0	80	58	50	29	17	14	59	3.5
Co/Al–Zr-02	0.05	81	64	–	60	38	–	59	3.5
Co/Al–Zr-05	0.13	90	67	58	63	37	18	64	3.8
Co/Al–Zr-11	0.26	98	65	–	62	39	–	64	3.8
Al–Zr-11	NA	0	0	0	0	0	0	0	0

[a] The ***RP*** and ***R_WP*** samples were re-calcined at 300 °C in air for 2 h before TPR measurement.
[b] The reducibility was based on a calibration with Ag_2O (100% reducibility).
[c] Error = ±5% of measurement of reducibility, as determined directly.
[d] The reducibility during TPR between 30 and 400 °C is related to the reducibility of the catalysts during standard reduction [23].
[e] Error = ±5% of measurement of H_2 chemisorption, as determined directly.
[f] %Co dispersion (%) = [2 × (total H_2 chemisorption/g cat)/(no. of μmol of Co total/g cat)] × 100%.

Table 5 shows the SSITKA results for Co catalysts with and without Zr modification. The surface reaction residence time for the CH_4 intermediates (τ_M) remained unchanged with Zr modification. Thus, there was no change in the intrinsic activity ($1/\tau_M$) of the methane-producing sites. This indicates that the mean activity of the sites producing methane was not affected by Zr modification. The surface residence time for CO (τ_{CO}) was also found to show no significant difference. The surface abundance of intermediates leading to the formation of methane (N_M), however, was almost twice as much upon Zr modification. The surface coverages for methane intermediates (θ_M) were found to be low (< 0.2), as is typical, but this was somewhat higher with Zr modification.

4. Discussion

It is obvious that Zr modification resulted in significant differences in the properties of alumina-supported Co. It was found that the reducibility for TPR from 30 to 800 °C (Table 2) increased somewhat with Zr modification (ZrO_2 = 2–11 wt%). However, and more importantly, the reducibility achieved during TPR from 30 to 400 °C (related to the reducibility during standard reduction at 350 °C for alumina-supported Co catalysts [23]) increased more significantly with Zr modification, although the amount of Zr added did not seem to have a great impact.

It is known from our previous work [38] that a high partial pressure of water vapor during reduction results in a lower reducibility for an unpromoted Co catalyst. Water present in the H_2 reduction gas (such as naturally occurs as a byproduct of metal catalyst reduction) decreases the reducibility of Co catalysts due to the formation of nonreducible (at temperatures $\leqslant$ 900 °C) Co "aluminate" [23,38], as is apparent in Table 2 for the unpromoted Co catalyst. This was also true for the Zr-modified catalysts. The reducibility (30–400 °C) of Co/Al–Zr-05-***RPC*** decreased from 37 to 18% (Table 2) when water was added during standard reduction (***R_WPC*** sample). However, it is obvious that the reducibility was still higher than that of unpromoted Co catalyst reduced also in the presence of water vapor (Co/Al-***R_WPC*** sample). In addition, as seen in Figs. 3 and 4, there was no Raman evidence for the formation of Co "aluminate" for the Zr-modified catalysts. This suggests that Zr modification

Table 3
FTS reaction rate and product distribution

Catalyst samples	Rate of CO conversion[a,b] (μmol/g cat/s)		TOF_H[c] × 10^3 (s^{-1})		Product distribution (wt%)					Carbon content (wt%)[d]
	Initial	SS	Initial	SS	C_1	C_2–C_4	C_5–C_{12}	C_{13+}	α	
Co/Al-***R***	3.0	2.2	25	19	14.2	48.0	35.9	1.9	0.63	0.42
Co/Al–Zr-02-***R***	6.5	3.6	55	31	11.0	42.5	42.5	4.0	0.66	–
Co/Al–Zr-05-***R***	7.5	3.6	59	28	11.3	43.1	41.9	3.7	0.66	0.14
Co/Al–Zr-11-***R***	6.5	3.8	51	30	11.1	42.7	42.3	3.9	0.68	–

[a] FTS was carried out at 220 °C, 1 atm, and H_2/CO ratio = 2 (H_2/CO/Ar = 60/30/10 cc/min). Catalyst samples were reduced (***R***) after pretreatments prior to the reaction.
[b] Error ± 5%, as determined directly.
[c] Based on total H_2 chemisorption.
[d] Carbon content on the used catalyst samples after FTS for 24 h was analyzed using combustion/colometric titration by Galbraith Laboratories, Inc.

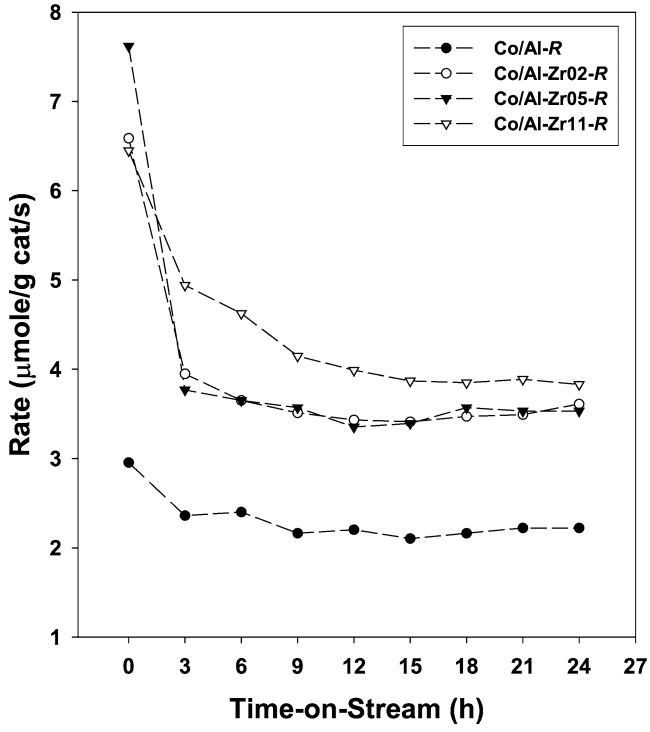

Fig. 10. Reaction rate vs TOS.

decreased the impact of water vapor during reduction, possibly by partially blocking Co "aluminate" formation.

In general, most authors have reported reducibilities during TPR of Co catalysts in the calcined form. For catalysts prepared with Co nitrate, TPR measurement of reducibilities of catalysts initially only calcined can result in an overestimation of the amount of Co reduced due to the consumption of H_2 by Co nitrate [3,38]. To eliminate this error, the residual nitrate has to be removed either by prolonging the initial calcination period from 2 to 14 h [3] or by reduction at 350 °C followed by re-calcination prior to TPR measurement. After the elimination of the Co nitrate peak at ca. 200 °C [3,38], only two reduction peaks remain [3,38]. This is the reason why reducibilities of the reduced, passivated, and recalcined samples are reported in this paper (Figs. 8 and 9) as they provide more accurate values of reducibility.

Table 4
Effect of pretreatment on reaction rate during FTS

Catalyst samples	Rate of CO conversion[a,b] (μmol/g cat/s)	
	Initial	Steady state
Co/Al-***R***	3.0	2.2
Co/Al-***RPR***	2.6	1.4
Co/Al-$\boldsymbol{R_W PR}$	2.2	0.6
Co/Al–Zr05-***R***	7.5	3.6
Co/Al–Zr05-***RPR***	6.5	2.2
Co/Al–Zr05-$\boldsymbol{R_W PR}$	5.0	1.8

[a] FTS was carried out at 220 °C, 1 atm, and H_2/CO ratio = 2 (H_2/CO/Ar = 60/30/10 cc/min). Catalyst samples were reduced after pretreatments prior to the reaction.
[b] Error ± 5%, as determined directly.

As reported by Rohr et al. [5], reducibilities of Co/γ-Al_2O_3 during TPR to 900 °C were not changed with Zr modification. Our measurements of reducibility were lower than those of Rohr et al., and we found that during TPR to 800 °C our Zr-modified catalysts exhibited slightly higher reducibilities than the unmodified one. The difference between our results and those of Rohr et al. was probably due to the fact that we eliminated the contribution from residual Co nitrate and TPR was performed to 800 °C. Probably because of the former, we were better able to detect important reducibility differences upon Zr modification.

In the present study, dramatic changes in the characteristics of the Raman bands for the reduced and passivated catalyst samples with Zr modification were observed. Basically, the Co "aluminate" bands were no longer present upon Zr modification. Only Raman bands for Co_3O_4 at 690, 480, and 198 cm^{-1} were evident on the reduced and passivated Zr-modified samples (Fig. 3). Similar results were also found even when water vapor was added during standard reduction, as shown in Fig. 4. This suggests that Zr modification decreases the amount of Co "aluminate" formed, even in the presence of water vapor. It should be noted, however, that XRD did not detect any differences upon Zr modification. The XRD results were typical for reduced Co/γ-Al_2O_3 catalysts [3,23,38]. The Co "aluminate" formed has been concluded to be too dispersed to be detected by XRD [38].

Table 5
SSITKA results for CO hydrogenation ($H_2/CO = 10$, $T = 220$ °C, and $P = 1.8$ atm)

Catalyst samples	CO conversion (%)	Rate of CO conversion (μmol/g cat/s)	Rate of CH_4 formation (μmol/g cat/s)	τ_{CO}[a] (s)	N_{CO}[b] (μmol/g cat)	τ_M[c] (s)	N_M[d] (μmol/g cat)	θ_M[e]	k_p[f] (s^{-1})	TOF_H[g] (s^{-1})
Co/Al	3.6	2.9	2.6	1.0	39	3.6	10	0.08	0.28	0.02
Co/Al–Zr11	7.0	5.5	4.9	1.0	41	3.5	17	0.13	0.28	0.04

[a] τ_{CO} = surface residence time of reversibly adsorbed CO. Standard deviation = ±0.2 s.
[b] N_{CO} = surface concentration of reversibly adsorbed CO. Standard deviation = ±2 μmol/g cat.
[c] τ_M = surface residence time of methane intermediates. Standard deviation = ±0.2 s.
[d] N_M = surface concentration of methane intermediates. Standard deviation = ±2 μmol/g cat.
[e] θ_M = surface coverage of carbonaceous methane intermediates = N_M/(total adsorbed H).
[f] $k_p = 1/\tau_M$, pseudo-first-order rate constant.
[g] TOF based on total H_2 chemisorption.

One of the most critical parameters determining the catalytic activity of Co FTS catalysts, besides Co reducibility, is H_2 chemisorption. However, it was found that the H_2 chemisorption on the reduced Co catalysts was not dramatically affected by Zr modification; there was only a slight increase in the amount of H_2 chemisorption (Table 2). Characterization of Co catalysts after FTS using hydrogen chemisorption is problematic since carbon deposited during FTS can interact with the hydrogen as well as cause spillover.

During FTS, the reaction rate declined on the average ca. 50% during time-on-stream to steady state (Fig. 10). This is typical for supported Co catalysts and is usually due to carbon deposition (see Table 3) that blocks the active sites. The initial activity of such catalysts can be usually largely recovered by extensive treatment with hydrogen or calcination/reduction.

Considering the unpromoted Co catalyst, its TOF was ca. 2×10^{-2} s^{-1}—typical for Co catalysts under these conditions. Due to the large increases in FTS rate without any changes in H_2 chemisorption, the calculated TOFs at steady-state based on H_2 chemisorption were found to be larger by a factor of 2 with Zr modification. Since TOF is basically related to the intrinsic activity by definition, it might appear that Zr modification caused an increase in the intrinsic activity for alumina-supported Co catalysts. However, this conclusion is rendered doubtful based on the SSITKA results.

Our SSITKA results confirm those of Rohr et al. [5] that the intrinsic activity is not affected by Zr modification, as indicated by the constant values of the intrinsic pseudo-first-order activity ($k_p = 1/\tau_M$). The SSITKA results show that there was an increase in the number of active reaction intermediates (N_M) with Zr modification. Thus, the higher activity of the Co catalysts with Zr modification was due either to a greater concentration of active sites or a higher occupancy of the sites during reaction. It is known that the number of active intermediates on the Co surface obtained by SSITKA during CO hydrogenation is only a small fraction ($\theta < 0.2$) of the number of Co metal surface atoms measured by H_2 chemisorption [2]. It should also be noted that the number of reaction intermediates is a better measure of the true number of active CO hydrogenation sites than is the number of reduced Co surface atoms obtained by H_2 chemisorption. Without any change in intrinsic activity, it is unlikely that an increase in surface coverage (θ) alone can explain the rate change, suggesting an increase in the number of active Co sites. Clearly, the reducibility of Co/γ-Al_2O_3 was increased by Zr modification, and it might be expected that H_2 chemisorption would also increase significantly. Given the consistency of the site activity ($1/\tau_M$), it is possible that TOF_H is in error (or at least variable) due to an incomplete chemisorption of H_2. The standard conditions for H_2 chemisorption on Co have been chosen to maximize activated chemisorption while minimizing hydrogen spillover. The conditions used, while appropriate for most Co catalysts, may not be appropriate for these Zr-modified ones.

5. Conclusions

Zr modification of the alumina support had a significant impact on the properties of Co/γ-Al_2O_3 catalysts. The overall catalytic activity during FTS increased significantly ($> 65\%$) upon Zr modification. SSITKA showed that the number of active reaction intermediates (N_M) increased with Zr modification while the intrinsic activity ($1/\tau_M$) remained constant. Most of this increase appears to have been due to an increase in reducibility during standard reduction. The increase in reducibility appeared to have been caused by a decrease in the amount of Co-SCF, as seen by Raman spectroscopy. Zr modification may have caused (i) a stabilization of the alumina support by blocking its defect sites, thus blocking Co "aluminate" formation, and/or (ii) a minimization of the impact of water vapor in modifying the surface properties of alumina, thereby decreasing the ease of Co reaction with the alumina. Thus, in summary, Zr modification increased Co reducibility and, probably, the number of exposed Co sites active for CO hydrogenation. Considering the variation in TOF_H but the lack of variation in $1/\tau_M$ (a measure of intrinsic activity), it is likely that TOF_H is in error due to errors in measuring accurately by H_2 chemisorption the number of reduced Co surface atoms. The standard H_2 chemisorption procedure of Reuel and Bartholomew [37] typically used by us and others, thus, may not be suitable for these Zr-modified Co catalysts.

Acknowledgments

The authors would like to thank the Royal Thai Government for financial support of B.J., Energy International, Inc., for providing the catalysts used in this study, and the Center for Advanced Engineering Fibers and Films (CAEFF) for the Raman spectrometer used in this study.

References

[1] E. Iglesia, S.L. Soled, F.A. Fiato, J. Catal. 137 (1992) 212.
[2] A.R. Belambe, R. Oukaci, J.G. Goodwin Jr., J. Catal. 166 (1997) 8.
[3] A. Kogelbauer, J.G. Goodwin Jr., R. Oukaci, J. Catal. 160 (1996) 125.
[4] S. Ali, B. Chen, J.G. Goodwin Jr., J. Catal. 157 (1995) 35.
[5] F. Rohr, O.A. Lindvag, A. Holmen, E.A. Blekkan, Catal. Today 58 (2000) 247.
[6] G.J. Haddad, B. Chen, J.G. Goodwin Jr., J. Catal. 160 (1996) 43.
[7] V.H.F.J. Blik, D.C. Köningsberger, R. Prins, J. Catal. 97 (1986) 210.
[8] J.H.A. Martens, V.H.F.J. Blik, R. Prins, J. Catal. 97 (1986) 200.
[9] V.H.F.J. Blik, R. Prins, J. Catal. 97 (1986) 188.
[10] M.A. Stranick, Houalla, D.M. Hercules, J. Catal. 104 (1987) 396.
[11] D. Schanke, S. Vada, E.A. Blekkan, A.M. Hilmen, A. Hoff, A. Holmen, J. Catal. 156 (1995) 85.
[12] A. Lycourghiotis, C. Defosse, F. Delannay, J. Lemaitre, B. Delmon, J. Chem. Soc. Faraday Trans. 76 (1980) 1677.

[13] M. Houalla, J. Lemaitre, B. Delmon, J. Chem. Soc. Faraday Trans. 78 (1982) 1389.
[14] M. Houalla, F. Delannay, B. Delmon, J. Phys. Chem. 85 (1981) 1704.
[15] A. Cimino, M. Logcono, M. Schiavello, J. Phys. Chem. 79 (1975) 243.
[16] M. Lo Jacono, M. Schiavello, V.H.J. DeBeer, G. Minelli, J. Phys. Chem. 81 (1977) 1583.
[17] G. Muralidhar, F.E. Massoth, J. Shabtai, J. Catal. 85 (1984) 44.
[18] F.E. Massoth, G. Muralidhar, J. Shabtai, J. Catal. 85 (1984) 53.
[19] R.L. Chin, D.M. Hercules, J. Catal. 74 (1982) 121.
[20] B.K. Sharma, M.P. Sharma, S.K. Roy, S. Kumar, S.B. Tendulkar, S.S. Tembe, B.D. Kulkarni, Fuel 77 (15) (1998) 1763.
[21] A. Kogelbauer, J.C. Weber, J.G. Goodwin Jr., Catal. Lett. 34 (1995) 259.
[22] D. Schanke, A.M. Hilmen, E. Bergene, K. Kinnari, E. Rytter, E. Adnanes, A. Holmen, Catal. Lett. 34 (1995) 269.
[23] Y. Zhang, D. Wei, S. Hammache, J.G. Goodwin Jr., J. Catal. 188 (1999) 218.
[24] R. Riva, H. Miessner, R. Vitali, G.D. Piero, Appl. Catal. A 196 (2000) 111.
[25] R. Bechara, D. Balloy, J.Y. Dauphin, J. Grimblot, Chem. Mater. 11 (1999) 1703.
[26] M. Kraum, M. Baerns, Appl. Catal. A 186 (1999) 189.
[27] B. Ernst, S. Libs, P. Chaumette, A. Kiennemann, Appl. Catal. A 186 (1999) 145.
[28] J.M. Jablonski, M. Wolcyrz, L. Krajczyk, J. Catal. 173 (1998) 530.
[29] B. Ernst, A. Bensaddik, L. Hilaire, P. Chaumette, A. Kiennemann, Catal. Today 39 (1998) 329.
[30] H. Ming, B.G. Baker, Appl. Catal. A 123 (1995) 23.
[31] D. Schanke, A.M. Hilmen, E. Bergene, K. Kinnari, E. Rytter, E. Adnanes, A. Holmen, Energy Fuels 10 (4) (1996) 867.
[32] R.L. Chin, D.M. Hercules, J. Phys. Chem. 86 (1982) 360.
[33] L.B. Backman, A. Rautiainen, A.O.I. Krause, M. Lindblad, Catal. Today 43 (1998) 11.
[34] R.B. Greegor, F.W. Lytle, R.L. Chin, D.M. Hercules, J. Phys. Chem. 85 (1981) 1232.
[35] M.F. Post, S.T.B. Sie, European Patent Application, 0167,215 A2, 1985.
[36] A. Hoek, A.H. Joustra, J.K. Minderhould, M.F. Post, UK Patent Application, GB 2,125,062 A, 1983.
[37] R.C. Reuel, C.H. Bartholomew, J. Catal. 85 (1984) 63.
[38] B. Jongsomjit, J. Panpranot, J.G. Goodwin Jr., J. Catal. 204 (2001) 98.
[39] Z. Liu, L. Dong, W. Ji, Y. Chen, J. Chem. Soc. Faraday Trans. 94 (8) (1998) 1137.
[40] P. Arnoldy, J.A. Moulijn, J. Catal. 93 (1985) 38.
[41] A.M. Hilmen, D. Schanke, A. Holmen, Catal. Lett. 38 (1996) 143.
[42] S.L. Shannon, J.G. Goodwin Jr., Chem. Rev. 95 (1995) 677.